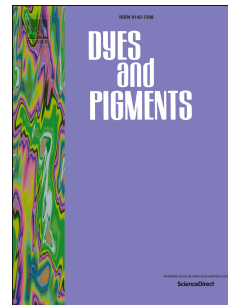


# Accepted Manuscript

Molecular design and synthesis of novel metal-free organic sensitizers with D- $\pi$ -A- $\pi$ -A architecture for DSSC application: The effect of the anchoring group

Mohamed R. Elmorsy, Rui Su, Ahmed A. Fadda, H.A. Etman, Eman H. Tawfik, Ahmed El-Shafei



PII: S0143-7208(18)30494-7

DOI: [10.1016/j.dyepig.2018.05.011](https://doi.org/10.1016/j.dyepig.2018.05.011)

Reference: DYPI 6740

To appear in: *Dyes and Pigments*

Received Date: 6 March 2018

Accepted Date: 7 May 2018

Please cite this article as: Elmorsy MR, Su R, Fadda AA, Etman HA, Tawfik EH, El-Shafei A, Molecular design and synthesis of novel metal-free organic sensitizers with D- $\pi$ -A- $\pi$ -A architecture for DSSC application: The effect of the anchoring group, *Dyes and Pigments* (2018), doi: 10.1016/j.dyepig.2018.05.011.

This is a PDF file of an unedited manuscript that has been accepted for publication. As a service to our customers we are providing this early version of the manuscript. The manuscript will undergo copyediting, typesetting, and review of the resulting proof before it is published in its final form. Please note that during the production process errors may be discovered which could affect the content, and all legal disclaimers that apply to the journal pertain.

with D- $\pi$ -A- $\pi$ -A Architecture for DSSC Application: The Effect of the Anchoring Group

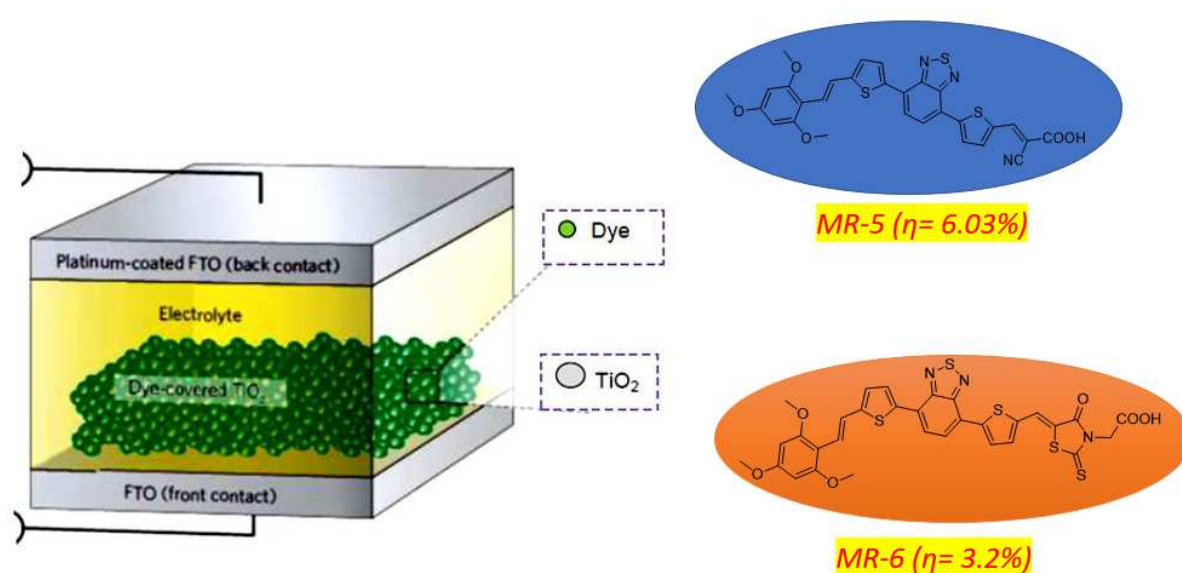
Mohamed R. Elmorsy<sup>a,b</sup>, Rui Su<sup>a</sup>, Ahmed A. Fadda<sup>b</sup>, H.A. Etman<sup>b</sup>, Eman H. Tawfik<sup>b</sup>, Ahmed El-Shafei<sup>a,\*</sup>.

<sup>a</sup>Polymer and Color Chemistry Program, North Carolina State University, Raleigh, NC, 27695, United States.

<sup>b</sup>Department of Chemistry, Faculty of Science, Mansoura University, El-Gomhoria Street, 35516 Mansoura, Egypt.

\* Corresponding author: E-mail: [Ahmed\\_El-Shafei@ncsu.edu](mailto:Ahmed_El-Shafei@ncsu.edu)

## GRAPHICAL ABSTRACT



## Abstract:

Herein, we report design and synthesis of two metal-free organic sensitizers (**MR-5** & **MR-6**) with D- $\pi$ -A- $\pi$ -A architecture based on trimethoxy benzene donor core carrying two different withdrawing/anchoring groups such as cyanoacetic acid and rhodanine-3-acetic acid

via thiophene as  $\pi$ -spacer. Benzothiadiazole was incorporated as an auxiliary acceptor, which greatly improved the molar extinction coefficient of the dyes. The optical and electrochemical properties of two dyes were investigated. The photovoltaic studies revealed that the dyes (**MR-5**) anchored with cyanoacetic acid showed significantly greater light harvesting (IPCE), which resulted in maximum PCE with good photovoltaic parameter than **MR-6**. **MR-5** achieved a better total solar-to-electric conversion efficiency of 6.03% and showed IPCE of 65% at 420 nm. Density functional theory (DFT) and time-dependent density functional theory (TD-DFT) calculations were used to study equilibrium molecular geometries and frontier molecular orbitals, and the data were consistent with experimental results.

**Keywords:** Trimethoxy benzene, D- $\pi$ -A- $\pi$ -A, Benzothiadiazole, DSSCs.

## 1. Introduction

Dye-sensitized solar cells (DSSCs) have been widely used due to their environmental friendliness, low-cost organic photovoltaics device with decent power conversion efficiency (PCE), as reported by O'Regan and Grätzel in 1991 [1]. Until now, the ruthenium complexes are investigated more as photo-sensitizer in the field of DSSCs because of their relatively good efficiency compared to normal silicon-based solar cells [2]. Two excellent dyes, **N719**  $\{(\text{Bu}_4\text{N})_2\text{Ru}[(4,4'\text{-CO}_2\text{H})_2\text{bipy}]_2(\text{NCS})_2\}$  and **N3**  $\{[\text{Ru}[(4,4'\text{-CO}_2\text{H})_2\text{bipy}]_2(\text{NCS})_2]\}$  have displayed maximum optimized PCE exceeding 11% [3-6]. In view of the low extinction coefficient of ruthenium photosensitizers, high manufacturing costs, multiple purification steps and rarity of the ruthenium metal, metal-free organic dyes attracted strong interest in the DSSCs community due to their advantages over metal based sensitizers [7].

One of the most successful design strategies of metal-free organic dyes represented as D- $\pi$ -A architectures due to their easy synthesis and reliable performance [7-10]. Recent activities have incorporated additional acceptor. In 2011, Zhu and Tian proposed a concept of a D-A- $\pi$ -A motif for designing a new generation of stable and efficient organic dyes [11-13]. From the literature reviews, some electron-withdrawing blocks, such as diketopyrrolopyrrole [14], benzotriazole [15] and benzothiadiazole, [16] have been employed to design D-A- $\pi$ -A framework. It is reported that additional acceptor is beneficial for extending absorption wavelength, modulating the energy levels, and thus greatly improving photovoltaic performances [13]. Furthermore, the evolution of  $\pi$ -bridge unit is essential in the molecular

engineering of sensitizers, which should be inserted as planar-type building blocks of fused heterocycles [17-19]. Many fused heterocycles such as benzene [19], thiophene [20], bithiophene [21] have been incorporated into the  $\pi$ -bridge with broad and intense spectral absorption in the visible-light region. So, extending the structure with  $\pi$ -spacer is beneficial to the enhancement of the photocurrent for efficient charge transfer [22]. Moreover, the most common electron withdrawing groups widely reported in the literature are cyanoacetic acid and rhodanine-3-acetic acid due to their strong electron withdrawing nature and effective binding on the surface of mesoporous  $\text{TiO}_2$  through carboxylic acid anchoring groups [23].

In this regard, in this present work, we have designed two D- $\pi$ -A- $\pi$ -A dyes (**MR-5** & **MR-6**) based on trimethoxy benzene core attached with different electron withdrawing groups such as cyanoacetic acid and rhodanine-3-acetic acid, respectively. In addition, thiophene ring was introduced to the dyes while the  $\pi$ -conjugated extension is an effective way to improve the short-circuit photocurrent density [24, 25]. Moreover, benzothiazole was also inserted into the structures due to their high chemical and photophysical stability [26, 27].

The designed organic dyes were synthesized from the 2,4,6-trimethoxybenzene with good yield following multi-step synthesis. The structures of target molecules **MR-5** and **MR-6** are shown in the Figure 1. The fabricated dyes and their intermediates were well-characterized using spectral techniques such as MS, FTIR, and  $^1\text{H}$  NMR analysis. Optical, photovoltaic, electrochemical and theoretical calculations of the synthesized dyes were studied. The results are subsequently elucidated in the following sections.

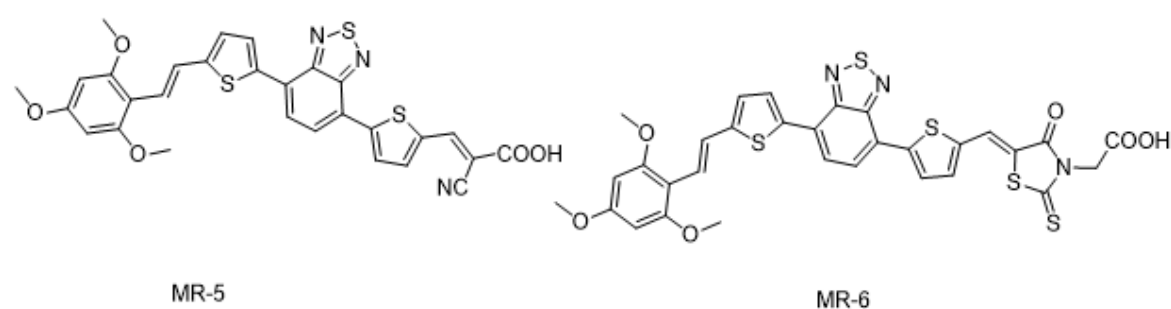


**Figure 1.** Molecular structure of **MR-5** and **MR-6**

## 2. Experimental

### 2.1. Materials and Methods

The solvents and chemicals were purchased from Sigma-Aldrich, Fisher Scientific, TCI-America or Ark Pharm and used as received. Sephadex LH-20 was purchased from Fisher Scientific. The mass spectrometry analysis was carried out on a high-resolution mass spectrometer, the Thermo Fisher Scientific Exactive Plus MS, a benchtop full-scan Orbitrap™ mass spectrometer using heated electrospray ionization (HESI). Samples were dissolved in methanol and sonicated for 15 min. They were then diluted 1:1 with 20 mM ammonium acetate and analyzed via syringe injection into the mass spectrometer at a flow rate of 10  $\mu\text{L}/\text{min}$ . The mass spectrometer was operated in positive ion mode. Fourier transform infrared spectroscopy (FT-IR) (ATR) spectra were recorded on a Nicolet Nexus 470 FT-IR spectrometer (Thermo Scientific, USA) and UV-visible spectra were measured by using Cary 300 spectrophotometer.  $^1\text{H}$  NMR spectra were recorded using a Varian 400 MHz spectrometer. Photovoltaic measurements of sealed cells were made by illuminating the cell through the conductive glass from the anode side with a solar simulator (WXS-155S-10) at AM 1.5 illuminations (light intensity: 100  $\text{mW cm}^{-2}$ ). IPCE measurements were made on a CEP-2000 system (Bunkoh-Keiki Co. Ltd.). EIS spectra were recorded over a frequency range of 100 mHz–200 kHz at 298 K. The applied bias voltage was set at the  $V_{oc}$  of the DSSCs, with AC amplitude set at 10 mV. The electrical impedance data were fitted using Z-Fit software (Bio-Logic). The procedure for DSSC fabrication is given in supporting information. The DFT calculations were performed using Gaussian09 package [28, 29] package.

### 2.2 Synthesis

The synthesis procedures were carried out using the standard synthetic methods. The synthetic procedure of the final compound and their intermediates with characterization data are given below.

#### 2.2.1 Synthesis of 5,5'-(benzo[c]thiophene-4,7-diyl) bis(thiophene-2-carbaldehyde) (1)

Compound **1** was synthesized with modification of the published procedure [30]. To a solution of 4,7-dibromobenzo[c]thiophene (294 g, 1.0 mmol), tetrakis(triphenylphosphine)palladium (115.53mg, 0.1mmol) in toluene (12 mL) were added ethanol (4 mL) solution of 5-

formylthiophene-2-ylbionic acid (400mg, 2.5mmol) and aqueous 2M sodium carbonate solution(5 mL) at room temperature under argon. After the mixture was heated at 50 °C for 4h, the reaction mixture was cooled, and the precipitate formed was filtered off, washed with water, methanol, and methylene chloride. The precipitate was further dried and collected as orange solid. The solid was purified by recrystallization with chloroform to give compound 1 with yield 60 %.

FT-IR: 1641.32 cm<sup>-1</sup> (-CHO stretch); ESI mass spectrum: C<sub>16</sub>H<sub>8</sub>N<sub>2</sub>O<sub>2</sub>S<sub>3</sub> [M+H] + Theo. M/Z = 356.698 [M+H] +, Found. M/Z 356.981.086, Error = -1.132 ppm.

#### **Synthesis of (2,4,6-trimethoxyphenyl) methanol (2):**

To a solution of NaBH<sub>4</sub> (160 mg, 4.2 mmol) in 30 ml dry dichloromethane and 10 mL anhydrous ethanol, 2,4,6-trimethoxybenzaldehyde (0.82 g, 4.2 mmol) was added rapidly and the bath was stirred at room temperature for 2h. The solution was poured into 50 ml water under vigorous stirring and then extracted with dichloromethane (15 mL). The organic layer was dried with anhydrous sodium sulfate and then rotary evaporated to remove the solvent and recrystallized using hexanes, to give **2** as a yellow solid.

<sup>1</sup>H NMR: (400 MHz, DMSO-*d*<sub>6</sub>) δ 6.24 (s, 2H), 4.80 (s, 2H), 3.82 (s, 6H), 3.75 (s, 3H). FT-IR: 3440.43 cm<sup>-1</sup> (-OH stretch); 2940.77, 2839.12 cm<sup>-1</sup> (-CH<sub>3</sub> stretch). ESI mass spectrum: C<sub>10</sub>H<sub>12</sub>O<sub>3</sub> [M+H] + Theo. M/Z = 181.086 [M+H] +, Found. M/Z 181.086, Error = 0.0145 ppm.

#### **Synthesis of bromotriphenyl(2,4,6-trimethoxybenzyl)-l5-phosphane (3)**

Compound **2** (0.75 g, 3.8 mmol) and PPh<sub>3</sub>·HBr (1.37 g, 4 mmol) were dissolved in 20 ml chloroform and refluxed for 2h. After removing the solvent, the residue was solidified with ether and filtrated to obtain compound **3** as a white solid.

<sup>1</sup>H NMR: (400 MHz, DMSO-*d*<sub>6</sub>) δ 7.46(dd, 6H), 7.35 (m, 9H), 6.13 (s, 2H), 3.82 (s, 6H), 3.78 (s, 3H), 2.60 (s, 2H). FT-IR: 2986.85, 2936.54 cm<sup>-1</sup> (-CH<sub>3</sub> stretch). ESI mass spectrum: C<sub>28</sub>H<sub>28</sub>O<sub>3</sub>P [M+] Theo. M/Z = 443.177 [M+], Found. M/Z 443.178, Error = 0.305 ppm.

#### **Synthesis of (E)-5-(7-(5-(2,4,6-trimethoxystyryl) thiophen-2-yl) benzo[c]thiophen-4-yl) thiophene-2-carbaldehyde (4)**

ACCEPTED MANUSCRIPT

The mixture of compound **1** (0.354g, 1 mmol), 18-crown-6 (15 mg, 0.05 mmol), K<sub>2</sub>CO<sub>3</sub> (276 mg, 2 mmol) was charged sequentially in a three-necked flask and then dried in vacuo for 30 min. A mixture of adduct **3** (0.523 g, 1.00 mmol) in dried DMSO (30 mL) was added dropwise to the mixture of over 3 h at 70 °C under N<sub>2</sub> atmosphere. The reaction mixture was stirred for a further 5 h at 70 °C, then was quenched with water and extracted with CH<sub>2</sub>Cl<sub>2</sub>. The organic layer was dried with anhydrous MgSO<sub>4</sub>. Silica gel chromatography with CH<sub>2</sub>Cl<sub>2</sub> gave aldehyde (**4**).

<sup>1</sup>H NMR: (400 MHz, DMSO-*d*<sub>6</sub>) δ 10.05 (s, 1H), 7.98 (d, 1H), 7.90 (d, 1H), 7.75 (d, 1H), 7.65 (d, 1H), 7.25 (d, 1H), 7.08 (d, 1H), 6.79 (d, 1H), 6.25 (s, 2H), 3.95 (s, 6H), 3.80 (s, 3H). FT-IR: 2960.25, 2927.73.13 cm<sup>-1</sup> (-CH<sub>3</sub> stretch), 1660.78 cm<sup>-1</sup> (-CHO stretch); ESI mass spectrum: C<sub>24</sub>H<sub>20</sub>O<sub>4</sub>S<sub>3</sub> [M+H]<sup>+</sup> + Theo. M/Z = 521.0658 [M+H]<sup>+</sup>, Found. M/Z 521.0652, Error = -0.987ppm.

**(Z)-2-cyano-3-(5''-(E)-2,4,6-trimethoxystyryl)-[2,2':5',2''-terthiophen]-5-yl) acrylic acid (MR-5)**

A mixture of aldehyde **4** (1.4g, 2.69mmol), cyanoacetic acid (0.265g, 3.12 mmol), ammonium acetate (2.2g, 2.85mmol), and glacial acetic acid (30 mL) was heated at 118 °C for 3h under N<sub>2</sub> atmosphere. The reaction mixture was allowed to cool to room temperature and then was quenched with water and extracted with CH<sub>2</sub>Cl<sub>2</sub>. The organic layer was washed with water and dried with anhydrous MgSO<sub>4</sub> and purified by silica gel chromatography with CH<sub>2</sub>Cl<sub>2</sub>: CH<sub>3</sub>OH (8:1) to yield **MR-5** as a deep red colored solid.

<sup>1</sup>H NMR (400 MHz, DMSO-*d*<sub>6</sub>) δ = 12.40 (s, 1H), 8.32 (s, 1H), 8.18 (s, thio-H), 8.16 (m, 2H, Ar-H), 7.63 (d, 1H, thio-H), 7.60 (d, 1H, thio-H), 7.28 (d, 1H, thio-H), 7.21 (d, 1H, thio-H), 6.31 (s, 2H, Ar-H), 3.91 (s, 6H, -CH<sub>3</sub>), 3.84 (s, 3H, -CH<sub>3</sub>); FT-IR: 2941.04, 2836.55 cm<sup>-1</sup> (-CH<sub>3</sub> stretch), 2213.35 cm<sup>-1</sup> (-CN stretch), 1706.27(-conjugated C=O stretch of -COOH); ESI-FTMS for C<sub>29</sub>H<sub>21</sub>N<sub>3</sub>O<sub>5</sub>S<sub>3</sub> [M+H]<sup>+</sup> + Theo. M/Z = 587.071 [M+H]<sup>+</sup>, Found. M/Z 588.071, Error = -1.695 ppm.

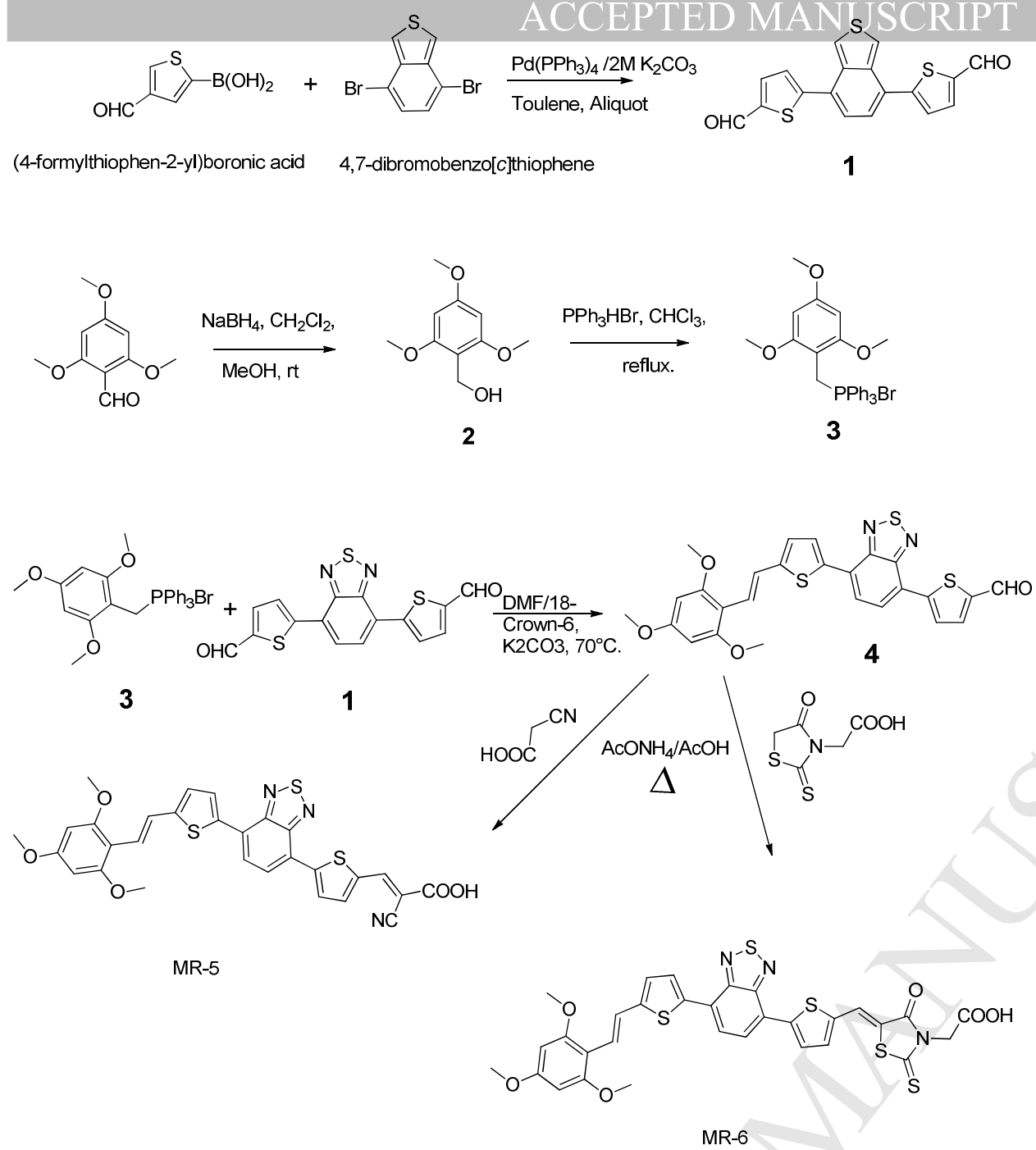
**2-((Z)-4-oxo-2-thioxo-5-(5''-(E)-2,4,6-trimethoxystyryl)-[2,2':5',2''-terthiophen]-5-yl) methylene) thiazolidin-3-yl) acetic acid (MR-6)**

A mixture of aldehyde **4** (1.4 g, 2.69 mmol), rhodanine-3-acetic acid (0.59 g, 3.12 mmol), and ammonium acetate (2.2 g, 2.85 mmol), dissolved in 30 mL of glacial acetic acid. The mixture was refluxed for 12 h under argon atmosphere. The progress of the reaction was monitored by TLC technique. After completion of the reaction, the content was cooled to room temperature, then it was poured into 100 g of crushed ice and the obtained red solid was filtered and dried. The product was purified by column chromatography using silica gel and CHCl<sub>3</sub>: CH<sub>3</sub>OH (5:1) as mobile phase to yield **MR-6** as pink colored solid

<sup>1</sup>H NMR (400 MHz, DMSO-*d*<sub>6</sub>)  $\delta$  = 12.85 (s, 1H, -COOH), 8.48 (s, 1H, =CH), 8.19 (s, 1H, thio-H), 8.16 (m, 2H, Ar-H), 7.64 (d, 1H, thio-H), 7.31 (d, 1H, thio-H), 7.28 (d, 1H, thio-H), 7.21 (d, 1H, thio-H), 5.21 (s, 1H, -CH<sub>2</sub>), 6.32 (s, 2H, Ar-H), 3.91 (s, 6H, -CH<sub>3</sub>), 3.80 (s, 3H, -CH<sub>3</sub>); FT-IR: 2965.99, 2938.87, 2835.18 cm<sup>-1</sup> (-CH<sub>3</sub> stretch), 1701.17 (C=O stretch) cm<sup>-1</sup>, 1723.59 (conjugated C=O stretch of -COOH); ESI-FTMS for C<sub>31</sub>H<sub>23</sub>N<sub>3</sub>O<sub>6</sub>S<sub>5</sub> [M+H]<sup>+</sup> Theo. M/Z = 694.026 [M+H]<sup>+</sup>, Found. M/Z = 694.025, Error = -1.532 ppm.

### 3. Results and Discussions

The synthetic pathways of two novel metal-free organic dyes **MR-5** and **MR-6** are depicted in Scheme 1. 5,5'-(benzo[c]thiophene-4,7-diyl) bis(thiophene-2-carbaldehyde) (**1**) was synthesized by Suzuki coupling of 4,7-dibromobenzo[c]thiophene with (4-formylthiophen-2-yl) boronic acid. After that compound **1** treated with a triphenyl phosphonium ylide adduct **3** through Wittig reaction to form the key precursor aldehyde **4** which synthesized in good yield. In the last step, the target sensitizers **MR-5** and **MR-6** were obtained in good yield by following Knoevenagel condensation of precursor **4** with cyanoacetic acid and rhodanine-3-acetic acid respectively. The target organic photosensitizers and their intermediates were purified using recrystallization and column chromatography techniques. The structures of the newly synthesized molecules and their intermediates were confirmed by various spectroscopic analysis.



**Scheme 1:** Synthesis of photosensitizer's **MR-5** and **MR-6**.

The absorption and emission spectra of the synthesized dyes were recorded in DMF ( $2 \times 10^{-5}$  M) solutions are depicted in Figure 2 and corresponding results are summarized in Table 1.

**Table 1** Absorption and emission properties for **MR-5** and **MR-6**.

Sensitizer	Absorption $\lambda_{\max}$ (nm)	$\epsilon$ ( $10^4 \text{M}^{-1} \text{cm}^{-1}$ )	Emission $\lambda_{\max}$ (nm)
MR-5	382; 545	5.05; 4.43	700
MR-6	368; 558	3.45; 4.64	708

From the absorption spectra, all dyes possess two distinctive bands. The band in the region of 360 to 400 nm are ascribed to the  $\pi$ - $\pi^*$  electron transitions of the conjugated molecules. The absorption band from (400-600 nm) is assigned to an intramolecular charge transfer (ICT) between the central unit and the anchoring moieties. The observed red shifted for both dyes due to the addition of the benzothiadiazole moiety. Whereas, compared to **MR-5**, **MR-6** showed a red shifted absorption, which can be attributed to the different structures of the anchoring group. From literature reviews, organic dyes with the same electron donor and  $\pi$ -conjugated spacer with rhodanine-3-acetic acid as electron acceptor compared to cyanoacetic acid anchoring moieties have better optical absorption properties [31, 32]. The molar extinction coefficient of dyes was found to be 4.43 and 4.64  $\text{M}^{-1} \text{cm}^{-1}$ , respectively indicating good light harvesting capability. Further, the emission spectra of **MR-6** was more red-shifted than that of **MR-5**.

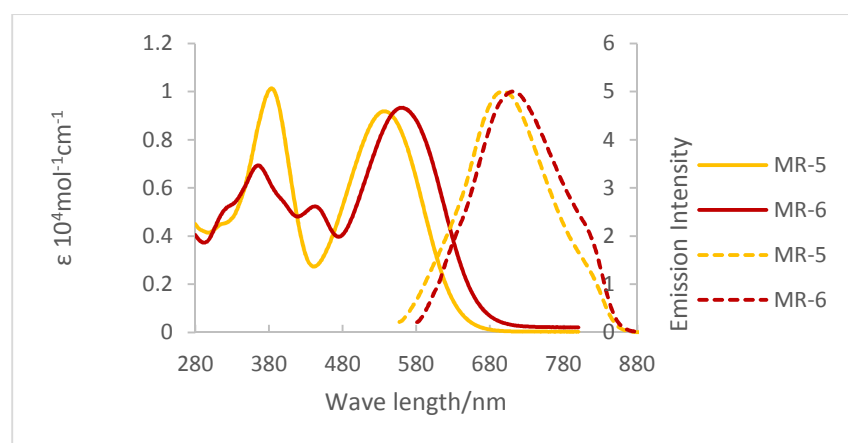


**Figure 2.** UV-Vis absorption (solid-line) and emission spectra (dashed-line) of **MR-5** and **MR-6** measured in DMF ( $2 \times 10^{-5}$  M).

The absorption spectra of **MR-5** and **MR-6** dyes adsorbed on TiO<sub>2</sub> film are displayed in **Figure 3**. As dyes adsorbed on the TiO<sub>2</sub> nanoparticle surface, the absorption spectra were red-shifted and broadened compared to the absorption spectra of the dye, indicating that majority of the dye molecules adsorbed on the TiO<sub>2</sub> surface. This broadening of the absorption spectra is due to an interaction between the dye and TiO<sub>2</sub> [33]. Moreover, **MR-5** found to be more adsorbed on TiO<sub>2</sub> surface compared to **MR-6**, which is an indication of the better performance of this dye.

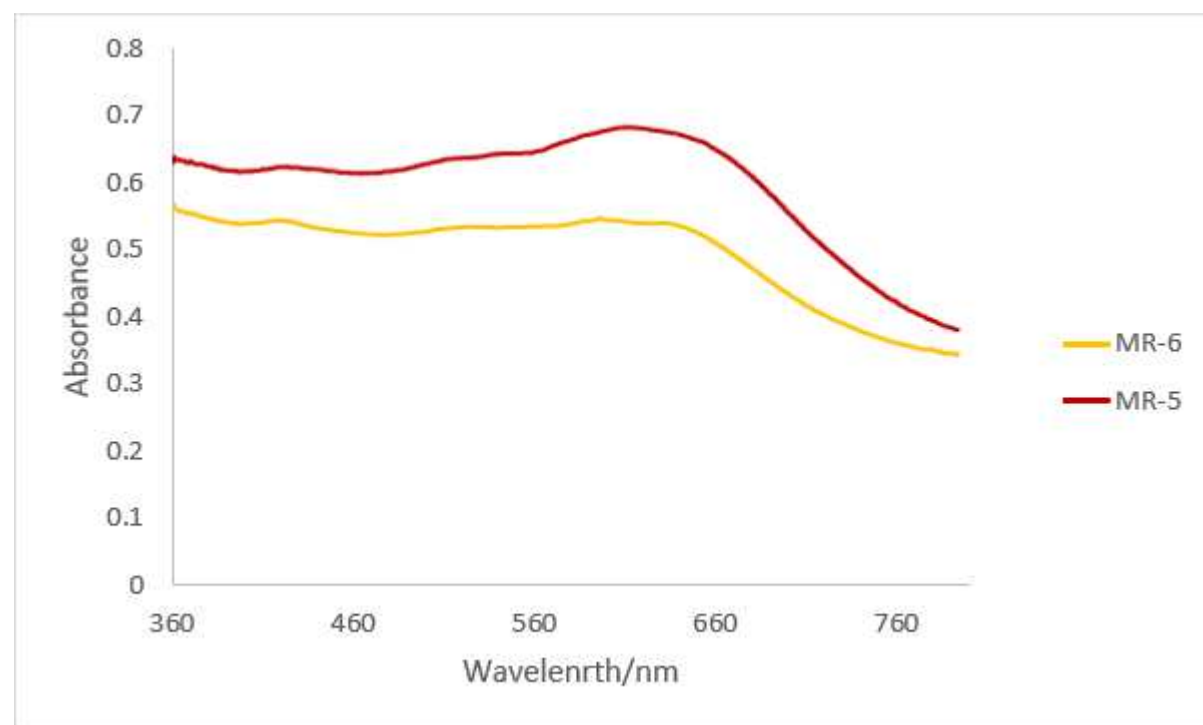


**Figure 3.** Absorption spectra of **MR-5** and **MR-6** adsorbed on nanoporous TiO<sub>2</sub>.

### 3.2. Electrochemical Characterization

Cyclic voltammetry (CV) studies were measured in DMF with the electrolyte 0.1 M [TBA][PF<sub>6</sub>] at a scan rate of 50 mV s<sup>-1</sup>. The working electrode used is the Glassy carbon, Pt wire represented the counter electrode and the reference electrode is Ag/Ag<sup>+</sup> in ACN. Fc/Fc<sup>+</sup> was introduced as an internal reference. The voltage measured was converted to NHE by addition value of 0.63 V. Fig. 1(b) shows the CV profile of **MR-5** and **MR-6**. The attained CV data were used to calculate the GSOP/HOMO energy level from onset oxidation potential of oxidation peak using the equation [34] (1)

$$\text{GSOP} = - [E_{\text{onset}}^{\text{oxd}} + 4.7\text{eV}] \dots\dots\dots (1)$$

Additionally,  $E_{0-0}$  (energy between the ground and excited states) which is the difference between HOMO and the first excited singlet was determined from the intersection of the absorbance and emission spectra. The optical band-gap  $E_{0-0}$  and GSOP values were employed to calculate their excited state oxidation potential (ESOP); the values in volts (V) against NHE were converted to electron volt (eV) according to the equation (2):

$$\text{ESOP} = [\text{GSOP} - E_{0-0}] \text{eV} \dots\dots\dots (2)$$

Figure 4 depicts the energy level diagram of the dyes. The calculated GSOP level of dyes **MR-5** (-5.47 eV) and **MR-6** (-5.57 eV) were found to be lower than that of the redox potential of  $\text{I}_3^-/\text{I}^-$  electrolyte system (-5.2 eV), demonstrating that there is enough thermodynamic driving force to regenerate the dye [35]. Moreover, estimated ESOP levels were found to be in order of **MR-5** (-3.54 eV) and **MR-6** (-3.56 eV) which were found to be higher than the conduction band edge of  $\text{TiO}_2$  (-4.2 eV), which shows that the electron injection from the synthesized dyes into the conduction band edge of  $\text{TiO}_2$  semiconductors is thermodynamically favorable [36]. Furthermore, **MR-5** has a larger electron injection potential than **MR-6**, indicating that the light-excited electrons are injected more efficiently in case of **MR-6**. Therefore, it is expected that **MR-5** carrying cyanoacetic acid as anchoring group will be more efficient for electron injection into the CB of  $\text{TiO}_2$  than the **MR-6**. Both **MR-5** and **MR-6** dyes meet the thermodynamic requirements for electron injection and dye regeneration process in the fabricated devices [37].

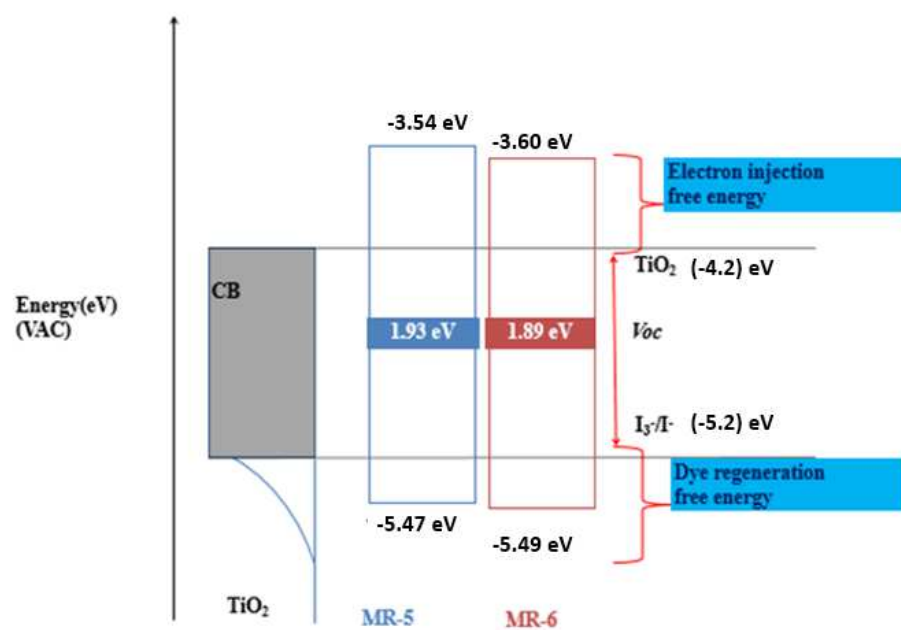


**Figure 4.** Energy level diagram and comparison between the GSOP and the ESOP of **MR-5** and **MR-6**.

### 3.4. TiO<sub>2</sub> electrode preparation and device fabrication

TiO<sub>2</sub> electrode preparation and DSSC devices fabrications with detailed procedure are provided in supplementary information

### 3.5. Photovoltaic and Electron impedences studies

The photo-voltaic performance of the DSSCs device fabricated using dyes **MR-5** and **MR-6** on mesoporous TiO<sub>2</sub> electrode in presence of 10 mM CDCA co-adsorbent were studied using standard AM 1.5 illuminations (light intensity: 100 mW cm<sup>-2</sup>) [38-40]. The procedure employed for the fabrication of devices are well explained in the electronic supplementary section. Figure 5 reveals the *J-V* characteristic curve of the photovoltaic devices and their detailed photovoltaic parameters were summarized in Table 2.

**Table 2.** I-V characteristics of solar devices based on **MR-5** and **MR-6**

Sensitizer	CDCA (mM)	$J_{SC}$ (mA·cm <sup>-2</sup> )	$V_{OC}$ (V)	FF (%)	$\eta$ (%)
MR-5	10	15.27	0.61	65.12	6.03
MR-6	10	8.7	0.56	64.65	3.2

Conditions: sealed cells; coadsorbate, CDCA 10 mM; photoelectrode, TiO<sub>2</sub> (15  $\mu$ m thickness and 0.18 cm<sup>2</sup>); electrolyte, 0.6 M DMPII, 0.1 M LiI, 0.05 I<sub>2</sub> in HI-30; irradiated light, AM 1.5 solar light (100 mW cm<sup>-2</sup>).  $J_{SC}$ , short-circuit photocurrent density;  $V_{OC}$ , open-circuit photovoltage; FF, fill factor;  $\eta$ , total power conversion efficiency.

The cell based on the dye **MR-5** showed the highest efficiency ( $\eta$ ) of 6.03 % ( $J_{SC} = 15.27$  mA/cm<sup>2</sup>,  $V_{OC} = 0.606$  V,  $FF = 65.12$ ) than **MR-6**. However, where **MR-6** showed an efficiency ( $\eta$ ) of 3.2 % ( $J_{SC} = 8.7$  mA/cm<sup>2</sup>,  $V_{OC} = 0.56$  V,  $FF = 64.65$ ). It was observed that both the short-circuit photocurrent ( $J_{SC}$ ) and the open-circuit voltage ( $V_{OC}$ ) for DSSC based on **MR-5** dye are higher than that of **MR-6** under the same experimental conditions. This improvement in  $V_{OC}$  contributed to the increase in electron lifetime in the DSSC by preventing the dark current, which will be discussed later in the impedance studies section. The higher ESOP level of **MR-5** is also supportive for the higher value of  $V_{OC}$  [41]. The increase in  $J_{SC}$  may be related to the higher amount of **MR-5** dye adsorbed on the TiO<sub>2</sub> nanocrystalline surface as compared to **MR-6** as shown in Figure 3. This increased surface area affords additional absorption sites for the dye, which correlates with better light harvesting efficiency of the photoelectrode **resulting** in an improvement in  $J_{SC}$ .

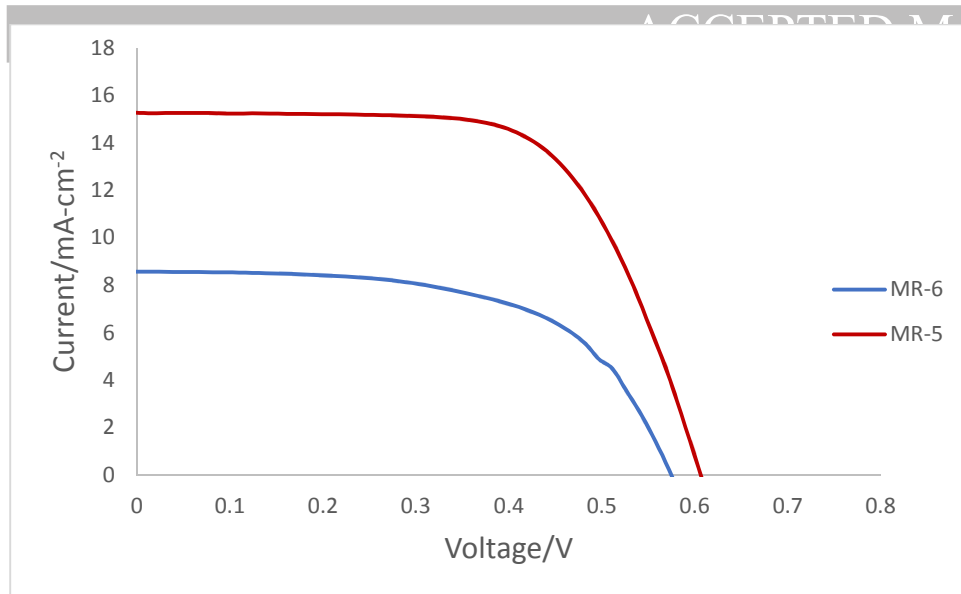
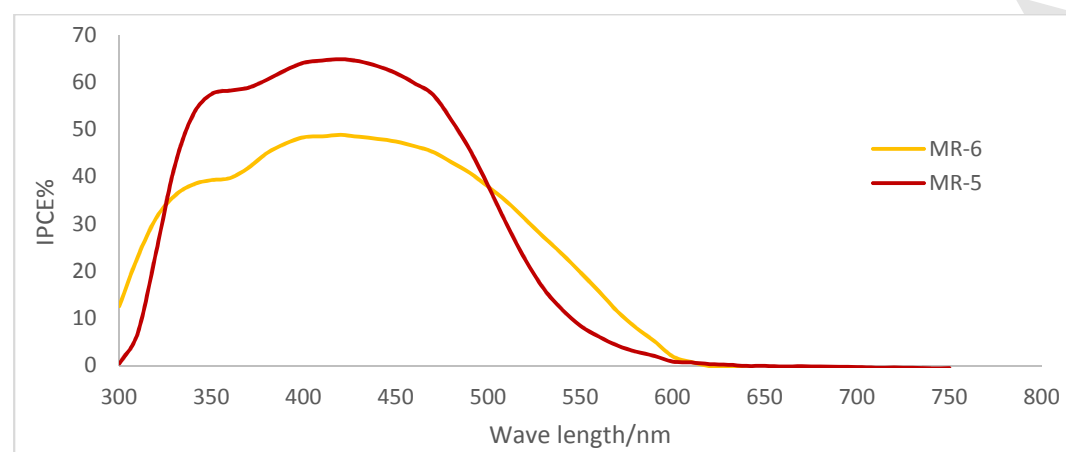


**Figure 5.** *I-V* characteristics of solar devices based on **MR-5** and **MR-6**.

Furthermore, the IPCE of **MR-5** was 57% at 350 nm and 65% in the range from 430 to 520 nm as shown in Figure 6. However, **MR-6** displayed a red-shifted expanding to 600nm but the top value reached only 49%. The observed low PCE value of **MR-6** may be related to the separation of LUMO level from the anchoring group of the dye due to the presence of methylene group which causes breakage in the  $\pi$ -conjugation and so, causing an inefficient electron injection from the photoexcited dye into the conduction band (CB) edge of  $\text{TiO}_2$ , resulting lower value of  $J_{SC}$ . With the aforementioned in mind, it is clear that the photovoltaic performances of the DSSCs are affected by the nature of the acceptor groups on the designed dyes. This agrees with the results of phenothiazine-based dyes reported by Tian et al. [42, 43].



Furthermore, electrochemical impedance spectroscopy (EIS) is used to evaluate the charge transfer, electron lifetime and chemical capacitance at the interface of  $\text{TiO}_2/\text{dye}/\text{electrolyte}$  and  $\text{pt}/\text{electrolyte}$  in the fabricated DSSC under practical conditions [44-46]. In general, the electrons are transported through the  $\text{TiO}_2$  nanoparticles to the electrolyte. The smaller the radius of the intermediate frequency semicircle in the Nyquist plot, the lower the electron transport resistance. On the other hand, the higher the charge recombination resistance in the Nyquist plot, the higher the photovoltic obtained from the fabricated solar cells, resulting in a higher  $e\text{TiO}_2$  lifetime [47, 48]. Figure 7 shows the Nyquist plots of DSSCs sensitizers with metal-free dyes-based cells, which reflects the electron recombination resistance, was found to be in order of **MR-5** > **MR-6** which is in good agreement with the  $V_{oc}$  of the devices.

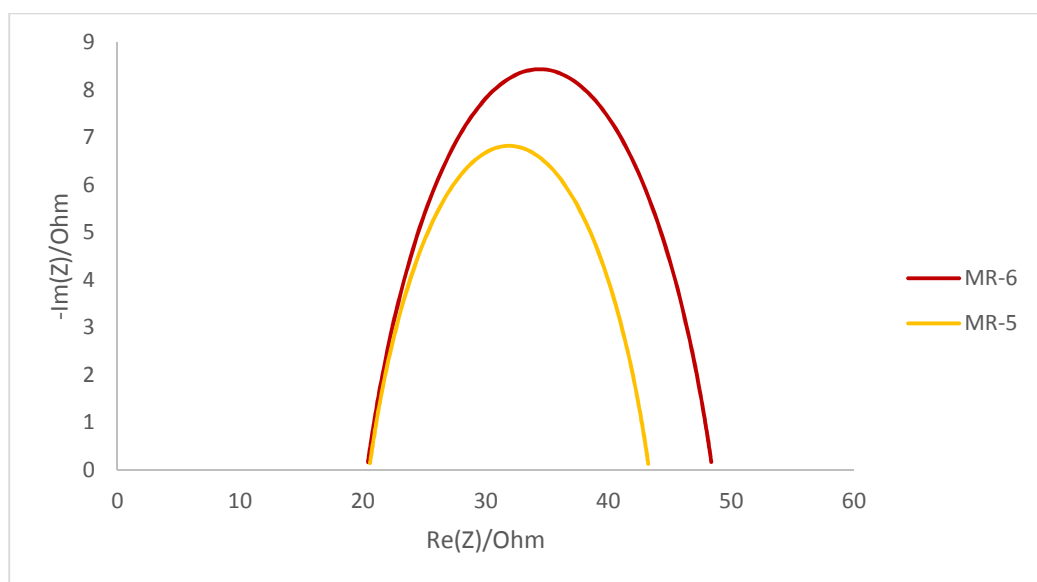


**Figure 7.** EIS Nyquist plots for solar devices based on **MR-5** and **MR-6**.

Moreover, the Bode plots, shown in Figure 8 can be used to evaluate  $e\text{TiO}_2$  (injected electrons in the conduction band of  $\text{TiO}_2$ ) by using the relation ( $\tau_{\text{eff}} = 1/2\pi f$ ), where  $\tau_{\text{eff}}$  is the lifetime of electrons in  $\text{TiO}_2$  and  $f$  is the midpoint frequency from Bode plot. Higher  $e\text{TiO}_2$  leads to improved  $V_{oc}$ . The lifetime in CB edge of  $\text{TiO}_2$  of the fabricated devices was found to be in

the order of **MR-5** > **MR-6**. From the later results, it is observed that **MR-5** has the highest  $e\text{TiO}_2$ , which means the highest  $V_{OC}$ .

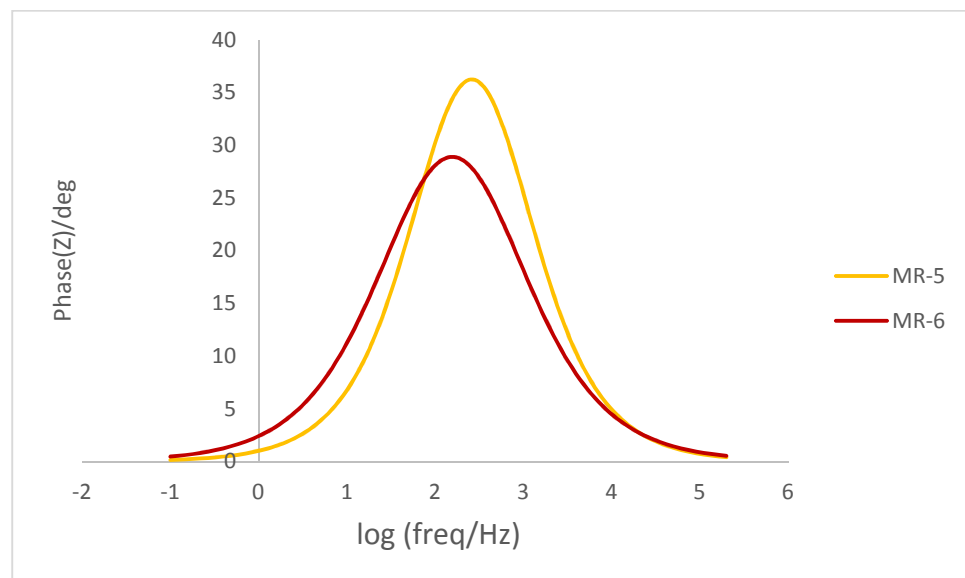


**Figure 8.** EIS Bode plots for solar devices based on **MR-5** and **MR-6**.

### 3.6 Molecular modeling

DFT calculations, implemented in Guassian09 package [28, 29], were performed on **MR-5** and **MR-6**. First, the ground-state geometries were optimized using DMF as a solvent, with B3LYP as energy functional and 6-31g (d, p) basis set. These optimized geometries were successively introduced to the TD-DFT energy calculation using the same energy functional and basis set.  $E_{0-0}$ , the optical energy gap, the ground and excited state oxidation potentials were calculated and are shown in **Table 3**, which were in good agreement with the experimental data.

**Table 3:** Excited state oxidation potential, and the lowest electronic transitions ( $E_{0-0}$ ) for **MR-5** and **MR-6**.

Sensitizer	Experimental (eV)			Theoretical (eV), TD-DFT <sup>d</sup>		
	$E_{0-0}$ <sup>b</sup>	GSOP (HOMO) <sup>a</sup>	$E^*$ (ESOP) <sup>c</sup>	$E_{0-0} = (S_0 - S_1)$	$E_{HOMO}$	ESOP <sub>singlet</sub>
MR-5	1.93	-5.47	-3.54	1.85	-5.48	-3.63
MR-6	1.89	-5.49	-3.60	1.74	-5.68	-3.88

[a] Oxidation potentials of dyes were measured in DMF with 0.1m [TBA][PF6] and at a scan rate of 50 mVs-1. They were calibrated with Fc/Fc+ as internal reference and converted to the NHE scale by addition of 0.63 V. [b]  $E_{0-0}$  was determined from the intersection of the absorption and tangent of the emission peak in DCM [25]. [c]  $E^*$  was calculated as  $E^*_{ox} - E_{0-0}$ . GSOP=ground state oxidation potential= EHOMO. Theoretical calculations based on B3LYP/ 6-31g (d, p) level DFT and TD-DFT calculations were given in parenthesis

The isodensity plots of frontier molecular orbitals (FMO) of **MR-5** and **MR-6** are displayed in Figure 9. As evidenced from their HOMO energy level, **MR-5** dye show push-pull electron effects, where the HOMO and the LUMO are mainly composed of donor and acceptor moieties, respectively. The HOMO is mainly localized on the trimethoxy benzene units (donors) and thiophene rings, and the LUMO is effectively delocalized on the benzothiadiazole and cyanoacetic acid units (acceptors). In the case of **MR-6**, the LUMO isosurface is mainly delocalized on the rhodanine-3-acetic acid moiety, particularly on the thiocarbonyl and carbonyl and thus resulting in the separation of LUMO from the anchoring moiety and, thus, preventing better injection of electrons into CB edge of TiO<sub>2</sub> [49]. Additionally, in **MR-6**, the dihedral angle between the -COOH acceptor/anchoring group and the rhodanine moiety is 75.66°, meaning that the anchoring group and the D- $\pi$ -A- $\pi$ -A scheme of the dye is not coplanar. As a consequence, the conjugation system is obstructed, and the electrons are partially delocalized, leading to inefficient photoexcitation upon light explosion, which decreases the electron injection from **MR-6** into the semiconductor and the final photovoltaic performance. However, it is coplanar in the case of **MR-5**, favoring efficient electron injection into TiO<sub>2</sub> (Figure 9b, d), which is also good evidence of the deficient performance of the dye **MR-6** bearing rhodanine-3-acetic acid as an anchoring group.

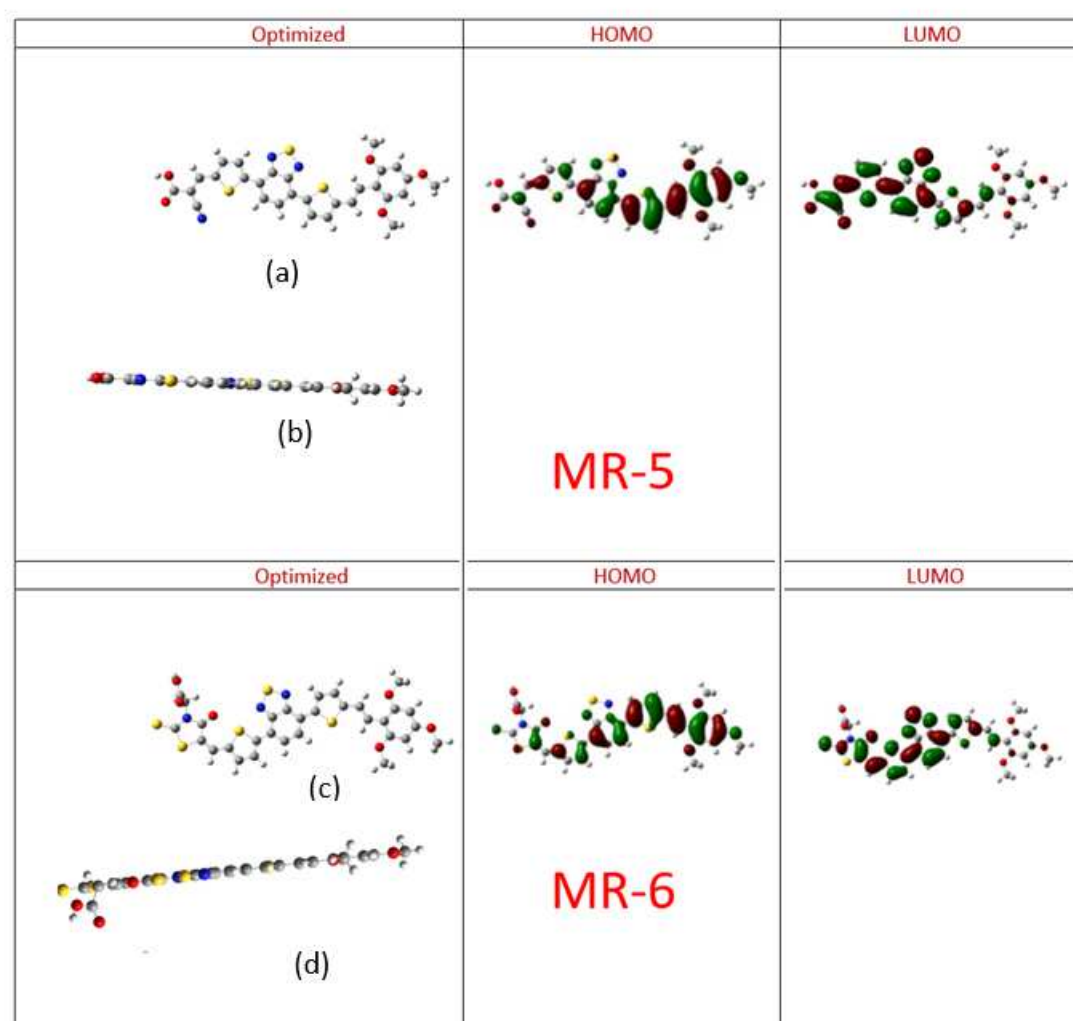


**Figure 9** Calculated isodensity of frontier occupied and unoccupied molecular orbitals for MR-5 and MR-6.

#### 4. Conclusion

We have successfully synthesized two novel D- $\pi$ -A- $\pi$ -A architecture metal-free organic dyes for DSSC application. Addition of benzothiazole unit as electron-acceptor next to the anchoring moiety provided strong electronic coupling between HOMO/LUMO, which translated to better DSSCs performance. **MR-6** showed a red shifted absorption, which can be attributed to the greater conjugation of the 4-oxo-2-thioxothiazolidine ring compared with the cyanoacetic unit. All the dyes possess the thermodynamical requirements for electron injection

into the conduction band edge of TiO<sub>2</sub> and dye regeneration of the electrolyte species. The device fabricated with MR-5 carrying cyanoacetic acid as anchoring moiety showed higher PCE of 6.03 %. Its  $J_{SC}$ ,  $V_{OC}$ , and IPCE values were found to be 15.27 mA/cm<sup>2</sup>, 0.606 V, and 65 %, respectively. The higher  $J_{SC}$  value indicated that, the dyes bearing cyanoacetic acid moiety as anchoring groups in the designed dyes bind efficiently on the surface of TiO<sub>2</sub> than the one containing rhodamine-3 acetic acid. Furthermore, from the electrochemical impedance spectroscopy (EIS), **MR-5** has longer electron lifetime (eTiO<sub>2</sub>), which means the highest  $V_{OC}$ , indicating good agreements with photovoltaic measurements. DFT studies indicate that rhodamine-3-acetic acid is poor anchoring group as in **MR-6** because the -COOH acceptor/anchoring group is almost at a 75.66° plane relative to the rhodamine ring which lowers the electron injection from **MR-6** into the CB edge of TiO<sub>2</sub>. Hence, the geometry of the anchoring group with respect to the chromophore is key in the efficiency of dye as a sensitizer for DSSCs.

## 5. Acknowledgements

The authors are thankful to the Department of Textile Engineering, Chemistry, and Science Department at NC State and the Egyptian Cultural and Educational Bureau, Washington D.C., for the financial support.

## 6. References

- [1] B. O'Regan, M. Grätzel, A low-cost, high-efficiency solar cell based on dye-sensitized colloidal TiO<sub>2</sub> films, *Nature*. 353 (1991) 737–740. doi:10.1038/353737a0
- [2] M. Grätzel, Recent Advances in Sensitized Mesoscopic Solar Cells, *Acc. Chem. Res.* 42 (2009) 1788–1798. doi:10.1021/ar900141y.
- [3] M.K. Nazeeruddin, P. Péchy, T. Renouard, S.M. Zakeeruddin, R. Humphry-Baker, P. Comte, P. Liska, L. Cevey, E. Costa, V. Shklover, L. Spiccia, G.B. Deacon, C.A. Bignozzi, M. Grätzel, Engineering of Efficient Panchromatic Sensitizers for Nanocrystalline TiO<sub>2</sub>-Based Solar Cells, *J. Am. Chem. Soc.* 123 (2001) 1613–1624. doi:10.1021/ja003299u.

- ACCEPTED MANUSCRIPT
- [4] A. Yella, C.-L. Mai, S.M. Zakeeruddin, S.-N. Chang, C.-H. Hsieh, C.-Y. Yeh, M. Grätzel, Molecular Engineering of Push–Pull Porphyrin Dyes for Highly Efficient Dye-Sensitized Solar Cells: The Role of Benzene Spacers, *Angew. Chem. Int. Ed.* 53 (2014) 2973–2977. doi:10.1002/anie.201309343.
- [5] (a) C.-Y. Chen, M. Wang, J.-Y. Li, N. Pootrakulchote, L. Alibabaei, C. Ngoc-le, J.-D. Decoppet, J.-H. Tsai, C. Grätzel, C.-G. Wu, S.M. Zakeeruddin, M. Grätzel, Highly Efficient Light-Harvesting Ruthenium Sensitizer for Thin-Film Dye-Sensitized Solar Cells, *ACS Nano*. 3 (2009) 3103–3109. doi:10.1021/nn900756s. (b) Y. Wang, X. Li, B. Liu, W. Wu, W. Zhu, Y. Xie, Porphyrins bearing long alkoxy chains and carbazole for dye-sensitized solar cells: tuning cell performance through an ethynylene bridge, *RSC Adv.* 3 (2013) 14780–14790. doi:10.1039/C3RA40788H. (c) Y. Tang, Y. Wang, X. Li, H. Ågren, W.-H. Zhu, Y. Xie, Porphyrins Containing a Triphenylamine Donor and up to Eight Alkoxy Chains for Dye-Sensitized Solar Cells: A High Efficiency of 10.9%, *ACS Appl. Mater. Interfaces*. 7 (2015) 27976–27985. doi:10.1021/acsami.5b10624.
- [6] S. Mathew, A. Yella, P. Gao, R. Humphry-Baker, B.F.E. Curchod, N. Ashari-Astani, I. Tavernelli, U. Rothlisberger, M.K. Nazeeruddin, M. Grätzel, Dye-sensitized solar cells with 13% efficiency achieved through the molecular engineering of porphyrin sensitizers, *Nature Chemistry*. 6 (2014) 242–247. doi:10.1038/nchem.1861.
- [7] A. Mishra, M.K.R. Fischer, P. Bäuerle, Metal-Free Organic Dyes for Dye-Sensitized Solar Cells: From Structure: Property Relationships to Design Rules, *Angewandte Chemie International Edition*. 48 (2009) 2474–2499. doi:10.1002/anie.200804709.
- [8] M.K.R. Fischer, S. Wenger, M. Wang, A. Mishra, S.M. Zakeeruddin, M. Grätzel, P. Bäuerle, D- $\pi$ -A Sensitizers for Dye-Sensitized Solar Cells: Linear vs Branched Oligothiophenes, *Chem. Mater.* 22 (2010) 1836–1845. doi:10.1021/cm903542v.
- [9] S. Hwang, J.H. Lee, C. Park, H. Lee, C. Kim, C. Park, M.-H. Lee, W. Lee, J. Park, K. Kim, N.-G. Park, C. Kim, A highly efficient organic sensitizer for dye-sensitized solar cells, *Chem. Commun.* (2007) 4887–4889. doi:10.1039/B709859F.
- [10] (a) Y. Wu, W. Zhu, Organic sensitizers from D- $\pi$ -A to D-A- $\pi$ -A: effect of the internal electron-withdrawing units on molecular absorption, energy levels and photovoltaic performances, *Chem. Soc. Rev.* 42 (2013) 2039–2058. doi:10.1039/C2CS35346F. (b) W. Li, J. Wang, J. Chen, F.-Q. Bai, H.-X. Zhang, Theoretical investigation of triphenylamine-

- based sensitizers with different  $\pi$ -spacers for DSSC, *Spectrochimica Acta Part A: Molecular and Biomolecular Spectroscopy*. 118 (2014) 1144–1151. doi:10.1016/j.saa.2013.09.080. (c) J. Sivanadanam, P. Ganesan, R. Madhumitha, M.K. Nazeeruddin, R. Rajalingam, Effect of  $\pi$ -spacers on the photovoltaic properties of D- $\pi$ -A based organic dyes, *Journal of Photochemistry and Photobiology A: Chemistry*. 299 (2015) 194–202.
- [11] Zhu W, Wu Y, Wang S, Li W, Li X, Chen J, Wang Z. Organic D-A- $\pi$ -A solar cell sensitizers with improved stability and spectral response. *Adv Funct Mater*, 2011, 21: 756–763
- [12] Pei K, Wu Y, Wu W, Zhang Q, Chen B, Tian H, Zhu W. Constructing organic D-A- $\pi$ -A-featured sensitizers with a quinoxaline unit for high-efficiency solar cells: The effect of an auxiliary acceptor on the absorption and the energy level alignment. *Chem Eur J*, 2012, 18: 8190–8200
- [13] Li W, Wu Y, Zhang Q, Tian H, Zhu W. D-A- $\pi$ -A featured sensitizers bearing phthalimide and benzotriazole as auxiliary acceptor: Effect on absorption and charge recombination dynamics in dye-sensitized solar cells. *ACS Appl Mater Inter*, 2012, 4: 1822–1830
- [14] S. Qu, B. Wang, F. Guo, J. Li, W. Wu, C. Kong, Y. Long, J. Hua, *Dyes and Pigments*, 92 (2012) 1384–1393.
- [15] J. Mao, F. Guo, W. Ying, W. Wu, J. Li, J. Hua, *Chem. Asian J.* 7 (2012) 982–991.
- [16] a) M. Velusamy, K. R. J. Thomas, J. T. Lin, Y. C. Hsu, K. C. Ho, *Org. Lett.* 2005, 7, 1899; b) J. Hou, H.-Y. Chen, S. Zhang, G. Li, Y. Yang, *J. Am. Chem. Soc.* 2008, 130, 16144; c) W. W. Li, C. Du, F. H. Li, Y. Zhou, M. Fahlman, Z. S. Bo, F. L. Zhang, *Chem. Mater.* 2009, 21, 5327; d) P. M. Beaujuge, W. Pisula, H. N. Tsao, S. Ellinger, K. Müllen, J. R. Reynolds, *J. Am. Chem. Soc.* 2009, 131, 7514; e) Z. M. Tang, T. Lei, K. J. Jiang, Y. L. Song, J. Pei, *Chem. Asia J.* 2010, 5, 1911.
- [17] M. Liang and J. Chen, *Chem. Soc. Rev.*, 2013, 42, 3453. Ragoussi, M. E.; Torres, T., New generation solar cells: concepts, trends and perspectives. *Chem. Commun.* 2015, 51, 3957-3972.
- [18] El-Sherbiny, D.; Cheema, H.; El-Essawy, F.; Abdel-Megied, A.; El-Shafei, A., Synthesis and characterization of novel carbazole-based terpyridyl photosensitizers for dye-sensitized solar cells (DSSCs). *Dyes and Pigments* 2015, 115, 81-87.

- [19] S. Ahmad, E. Guillen, L. Kavan, M. Grätzel and M. K. Nazeeruddin, *Energy Environ. Sci.*, 2013, 6, 3439.
- [20] M. Xu, M. Zhang, M. Pastore, R. Li, F. de Angelis and P. Wang, *Chem. Sci.*, 2012, 3, 976.
- [21] H. Qin, S. Wenger, M. Xu, F. Gao, X. Jing, P. Wang, S. M. Zakeeruddin and M. Grätzel, *J. Am. Chem. Soc.*, 2008, 130, 9202.
- [22] P. Gao, H. N. Tsao, M. Grätzel and M. K. Nazeeruddin, *Org. Lett.*, 2012, 14, 4330.
- [23] D.D. Babu, S.R. Gachumale, S. Anandan, A.V. Adhikari, New D- $\pi$ -A type indole based chromogens for DSSC: Design, synthesis and performance studies, *Dyes and Pigments*. 112 (2015) 183–191.
- [24] Iqbal Z, Wu W, Huang Z, Wang L, Kuang DB, Meier H, et al. Trilateral conjugation extensions of phenothiazine-based dyes enhance the photovoltaic performance of the dye-sensitized solar cells. *Dyes Pigments*. 2016;124: 63-71.
- [25] Iqbal Z, Wu W, Kuang DB, Wang L, Meier H, Cao D. Phenothiazine-based dyes with bilateral extension of p-conjugation for efficient dye-sensitized solar cells. *Dyes Pigments*. 2013; 96:722-731.
- [26] Hrobarikova V, Hrobarik P, Gajdos P, Fitolis I, Fakis M, Persephonis P, Zahradnik P. Benzothiazole-based fluorophores of donor- $\pi$ - acceptor- $\pi$ -donor type displaying high two-photon absorption. *J Org Chem*, 2010, 75: 3053–3068
- [27] Lartia R, Allain C, Bordeau G, Schmidt F, Fiorini-Debuisschert C, Charra F, Paule M, Teulade F. Synthetic strategies to derivatizable triphenylamines displaying high two-photon absorption. *J Org Chem*, 2008, 73: 1732–1744
- [28] Bomben, P. G.; Theriault, K. D.; Berlinguette, C. P., Strategies for Optimizing the Performance of Cyclometalated Ruthenium Sensitizers for Dye-Sensitized Solar Cells. *Eur. J. Inorg. Chem*. 2011, 1806-1814.
- [29] Frisch, M. J.; Trucks, G. W.; Schlegel, H. B.; Scuseria, G. E.; Robb, M. A.; Cheeseman, J.R.; Scalmani, G.; Barone, V.; Mennucci, B.; Petersson, G. A.; Nakatsuji, H.; Caricato, M.; Li, X.; Hratchian, H. P.; Izmaylov, A. F.; Bloino, J.; Zheng, G.; Sonnenberg, J. L.; Hada, M.; Ehara, M.; Toyota, K.; Fukuda, R.; Hasegawa, J.; Ishida, M.; Nakajima, T.; Honda, Y.; Kitao, O.; Nakai, H.; Vreven, T.; Jr; Peralta, J. E.; Ogliaro, F.; Bearpark, M.; Heyd, J. J.; Brothers, E.; J. Bisquert, Chemical capacitance of nanostructured semiconductors: its origin and significance for nanocomposite solar cells, *Phys. Chem.*

- [30] Xuelong Zhang,<sup>b</sup> Rumiko Yamaguchi,<sup>c</sup> Keiichi Moriyama,<sup>c</sup> Masami Kadowaki,<sup>d</sup> Takako Kobayashi,<sup>d</sup> Tsutomu Ishi-i,<sup>a</sup> Thies Thiemanna and Shuntaro Mataka, *Journal of Materials Chemistry*, 16(8),2006, 736-740.
- [31] P. Naik, R. Su, M.R. Elmorsy, A. El-Shafei, A.V. Adhikari, investigation of new carbazole based metal free dyes as active photo-sensitizers/cosensitizers for dye sensitized solar cells, *Dyes and Pigments*. 149 (2018) 177-187.
- [32] Modelli, A.; Jones, D.; Pshenichnyuk, S. A. Electron Attachment to Dye-Sensitized Solar Cell Components: Rhodanine and Rhodanine- 3-acetic Acid. *J. Phys. Chem. C* 2010, 114, 1725–1732.
- [33] K. Hara, M. Kurashige, Y. Dan-oh, C. Kasada, A. Shinpo, S. Suga, K. Sayama, H. Arakawa, *New J. Chem.* 27 (2003) 783.
- [34] Su, R.; Elmorsy, M. R.; Abed, M.; Islam, A.; Lord, M.; Fadda, A. A.; El-Shafei, A., A Comparative Study on Two Ru(II) Complexes with Thiophene-Based Ancillary Ligands for High-Efficiency Dye-Sensitized Solar Cells. *Eur. J. Inorg. Chem.*, 2017, 2017 (31), 3690-3697.
- [35] P. Qu, G.J. Meyer, Proton-controlled electron injection from molecular excited states to the empty states in nanocrystalline TiO<sub>2</sub>, *Langmuir* 17 (2001) 6720– 6728.
- [36] Gerko Oskam, V. Bryan Bergeron, J. Gerald Meyer, C. Peter Searson, Pseudohalogens for dye-sensitized Ti photoelectrochemical cells, *J. Phys. Chem. B* 105 (2001) 6867–6873.
- [37] H. Cheema, A. Islam, L. Han, A. El-Shafei, Influence of number of benzodioxan-stilbazole-based ancillary ligands on dye packing, photovoltage and photocurrent in dye-sensitized solar cells, *ACS Appl. Mater. Interfaces* 6 (2014) 11617–11624.
- [38] H. Cheema, A. Islam, R. Younts, B. Gautam, I. Bedja, R.K. Gupta, L. Han, K. Gundogdu, A. El-Shafei, more stable and more efficient alternatives of Z-907: carbazole-based amphiphilic Ru(II) sensitizers for dye-sensitized solar cells, *Phys. Chem. Chem. Phys.* 16 (2014) 27078–27087.
- [39] D.D. Babu, R. Su, A. El-Shafei, A.V. Adhikari, New indole based co-sensitizers for dye sensitized solar cells exceeding 10% efficiency, *RSC Adv.* 6 (2016) 30205– 30216.
- [40] Y. Wang, L. Xu, X. Wei, X. Li, H. Ågren, W. Wu, Y. Xie, 2- Diphenylaminothiophene as the donor of porphyrin sensitizers for dye-sensitized solar cells, *New J. Chem.* 38 (2014)

- [41] W. Xu, J. Pei, J. Shi, S. Peng, J. Chen, J. Power Sources 183 (2008) 792.
- [42] H. Tian, X. Yang, R. Chen, Y. Pan, L. Li, A. Hagfeldt, L. Sun, Phenothiazine derivatives for efficient organic dye-sensitized solar cells, Chem. Commun. (2007) 3741–3743.
- [43] H. Tian, X. Yang, R. Chen, R. Zhang, A. Hagfeldt, L. Sun, Effect of different dye baths and dye-structures on the performance of dye-sensitized solar cells based on triphenylamine dyes, J. Phys. Chem. C 112 (2008) 11023–11033.
- [44] Kern, R., et al., Modeling and interpretation of electrical impedance spectra of dye solar cells operated under open-circuit conditions. Electrochimica Acta, 2002. 47(26): p. 4213-4225.
- [45] Wang, Q., J.-E. Moser, and M. Grätzel, Electrochemical Impedance Spectroscopic Analysis of Dye-Sensitized Solar Cells. The Journal of Physical Chemistry B, 2005. 109(31): p. 14945-14953.
- [46] Koide, N., et al., Improvement of efficiency of dye-sensitized solar cells based on analysis of equivalent circuit. Journal of Photochemistry and Photobiology A: Chemistry, 2006. 182(3): p. 296-305.
- [47] Fabregat-Santiago, F., et al., Influence of electrolyte in transport and recombination in dye-sensitized solar cells studied by impedance spectroscopy. Solar Energy Materials and Solar Cells, 2005. 87(1–4): p. 117-131.
- [48] Cheema, H., et al., More stable and more efficient alternatives of Z-907: carbazole-based amphiphilic Ru(II) sensitizers for dye-sensitized solar cells. Phys Chem Chem Phys, 2014. 16(48): p. 27078-87
- [49] M. Matsui, A. Ito, M. Kotani, Y. Kubota, K. Funabiki, J. Jin, T. Yoshida, H. Minoura, H. Miura, The use of indoline dyes in a zinc oxide dye-sensitized solar cell, Dyes Pigments. 80 (2009) 233–238.